FhuF, Part of a Siderophore−Reductase System†

Berthold F. Matzanke,*,‡ Stefan Anemüller,§ Volker Schünemann,|| Alfred X. Trautwein,|| and Klaus Hantke*,⊥

Isotopenlabor TNF, Institut für Biochemie, and Institut für Physik, Universität zu Lübeck, Ratzeburger Allee 160, D-23538 Lübeck, Germany, and Mikrobiologie/Membranphysiologie, Eberhard-Karls Universität, Auf der Morgenstelle 28, D-72076 Tübingen, Germany

Received October 1, 2003; Revised Manuscript Received December 4, 2003

ABSTRACT: FhuF is a cytoplasmic 2Fe-2S protein of *Escherichia coli* loosely associated with the cytoplasmic membrane. *E. coli fhuF* mutants showed reduced growth on plates with ferrioxamine B as the sole iron source, although siderophore uptake was not defective in transport experiments. Removal of iron from coprogen, ferrichrome, and ferrioxamine B was significantly lower in *fhuF* mutants compared to the corresponding parental strains, which suggested that FhuF is involved in iron removal from these hydroxamate-type siderophores. A redox potential $E_{1/2}$ of -310 ± 25 mV relative to the normal hydrogen electrode was determined for FhuF by EPR redox titration; this redox potential is sufficient to reduce the siderophores coprogen and ferrichrome. Mössbauer spectra revealed that FhuF in its [Fe^{2+}-Fe^{3+}] state is also capable of direct reduction of ferrioxamine B-bound ferric iron, thus proving its reductase function. This is the first report on a bacterial siderophore−iron reductase which in vivo seems to be specific for a certain group of hydroxamates.

[Fe^{3+}] siderophores are a major source of iron in bacteria. Siderophores have a much lower affinity for Fe^{2+} than for Fe^{3+}, and the kinetics of ligand exchange of high-spin Fe^{2+} are much faster than for high-spin Fe^{3+} (*1*). Therefore, reduction of ferric siderophores accompanied by ligand exchange is an excellent mechanism for intracellular iron release. In fact, one main route of bacterial iron acquisition includes active transport of ferric siderophores across cell membranes, followed by intracellular iron removal from the siderophore carrier via reduction (*2*−*4*). The deferrated siderophore is rapidly excreted (*5*). Many flavin reductases have the property to reduce [Fe^{3+}] siderophores in vitro. However, surprisingly it is not known which enzymes reduce the [Fe^{3+}] siderophore in the cell (*2*).

Escherichia coli K-12 has an efficient hydroxamate siderophore uptake system that allows the utilization of ferrichrome and coprogen which are produced by fungi. Also ferrioxamine B, mainly produced by streptomyces, may be used; however, the amount of iron taken up via ferrioxamine B (FoxB)[1] is less than 5% of the amount observed for coprogen- or ferrichrome-mediated iron transport. Nevertheless, this low uptake eliminates iron-dependent growth limitation. Ferrioxamine B is mostly taken up across the outer membrane by the TonB-dependent receptor FhuE (*6*). Transport across the cytoplasmic membrane is exclusively dependent on the ABC transporter FhuCDB. However, the periplasmic binding protein FhuD has a very low affinity for ferrioxamine B (*7*). In addition, *fhuF* mutants exhibit a diminished ability to grow on plates with ferrioxamine B as the sole iron source, although no defect in siderophore uptake is observed. Moreover, these growth conditions lead to a derepression of various Fur-dependent iron transport systems. The function of FhuF is unclear.

Transcription of *fhuF* is derepressed by a low iron level in the cell via the iron regulator Fur and repressed by OxyR, an oxidative response regulator (*8*). The FhuF protein of *E. coli* contains a [2Fe-2S] cluster exhibiting the unusual cluster binding motif C-C-x_{10}-C-x-x-C (*9*). Moreover, the amino acid sequence of FhuF does not show any similarities to sequences of known [2Fe-2S] proteins.

The location of the FhuF protein in the cytoplasm, the presence of a [2Fe-2S] cluster in the FhuF, its regulation by iron, and the diminished ferrioxamine B utilization in an *fhuF* mutant has led to the assumption that the protein is involved in iron mobilization from ferrioxamine B, possibly as a siderophore−iron reductase (*9*).

In the present study, evidence for the siderophore−iron reductase function of FhuF was found by employing EPR redox titrations, Mössbauer spectroscopy, and [^{55}Fe] siderophore extraction experiments from *E. coli fhuF* mutants.

EXPERIMENTAL PROCEDURES

Strains and plasmids used are listed in Table 1. Strain H1608 was obtained by P1 transduction from *E. coli* ZI352 *fhuF*::MudX into *E. coli* AB2847 Δ(*pro lac*). In strain ZI352, Mu is located 698 bp behind the start codon of *fhuF* (*9*). Cells were grown in TY medium containing (per liter) tryptone (8 g), yeast extract (5 g), and sodium chloride (5 g) or in M9 medium (*10*). Growth response to ferrioxamine

† This work was supported by Grant HA1186 from the DFG to K.H.

* Corresponding authors. K.H.: Tel: +49-7071-2974645. Fax: +49-7071-5843. E-mail: hantke@uni-tuebingen.de. B.F.M.: Tel: +49-451-5004140. Fax: +49-451-5004139. E-mail: matzanke@physik.uni-luebeck.de.

‡ Isotopenlabor TNF, Universität zu Lübeck.

§ Institut für Biochemie, Universität zu Lübeck.

|| Institut für Physik, Universität zu Lübeck.

⊥ Mikrobiologie/Membranphysiologie, Eberhard-Karls Universität.

[1] Abbreviations: NHE, normal hydrogen electrode; Fhu, ferric hydroxamate uptake; FoxB, ferrioxamine B; EPR, electron paramagnetic resonance; BSA, bovine serum albumin; TonB, T-one resistance in *Escherichia coli*.

10.1021/bi0357661 CCC: $27.50
Published on Web 01/10/2004

Table 1: *E. coli* Strains and Plasmids Used in This Study

strain or plasmid	parent and relevant marker	ref
strain		
Bl21(DE3)	T7 polymerase on λDE3 under *lac*-UV5 control	*9*
MC4100	*araD131* Δ(*argF-lac*)205 *flhD5301 fruA25 relA1 rpsL150 rbsR22 deoC1*	*9*
H1443	same as MC4100 but *aroB*	*9*
H1717	same as H1443 but *fhuF-7*::λ*plac*Mu	*9*
AB2847	aroB malT tsx	*35*
H1085	same as AB2847 but *pepN*::MudX	*35*
H1004	same as H1085 but *fes*	*35*
H1608	same as AB2847 but Δ(*pro lac) fhuF*::MudX	this work
plasmid		
pKF191	*fhuF*$^+$	*9*
pFU2	*foxA*$^+$	*15*
pEN7	*iutA*$^+$	*7*

B was tested on nutrient broth dipyridyl plates (8 g of nutrient broth, 5 g of NaCl, 15 g of Difco agar/L, and 0.2 mM 2,2′-dipyridyl), which were seeded with the appropriate strain in 2.5 mL of soft agar in water. Filter paper disks impregnated with 15 μL of 2 mM ferrioxamine B were applied, and growth zones were measured after 18 h.

Transport Experiments. For iron uptake experiments, cells were grown in TY medium at 37 °C with 50 μM ethylenediaminedi(*o*-hydroxyphenylacetic acid) to derepress iron transport systems. Cells were harvested at an OD_{578} of 0.5−0.8 and washed with M9 transport medium (10 mL of 10× M9 salts, 1 mL of 0.1 M $MgSO_4$, 0.25 mL of 40% glucose, and 89 mL of deionized water) at 4 °C. Cells were resuspended in M9 transport medium to an OD_{578} of 1.0 and kept on ice; the cells were incubated with shaking at 30 °C for 5 min before the onset of transport. [$^{55}Fe^{3+}$] siderophore was added to a final concentration of 1 μM. After 16 min, 1 mL of the cell suspension was sedimented in 1.5 mL Eppendorf tubes and washed in 0.5 mL of M9 transport medium to remove adhering Fe siderophore. The sediment was resuspended in 50 μL of 5 M NaCl and extracted with 500 μL of benzyl alcohol. [^{55}Fe] in an aliquot of the benzyl alcohol extract and in whole cells was measured with a liquid scintillation counter. The percentage of extractable iron was determined.

Isolation of FhuF. FhuF protein carrying a His tag was isolated as reported earlier (*9*).

EPR Spectroscopy. Measurements were made at 30 K at X-band (9.63 GHz) using a conventional EPR spectrometer (Bruker ER200D) equipped with a helium-flow cryostat (Oxford Instruments ESR) (*12*). Data were acquired using a personal computer and a program developed in our laboratories.

EPR Redox Titration. Potentiometric redox titrations were performed in 50 mM Tris-HCl, pH 7.3, under anaerobic conditions as described by Dutton (*11*). The redox mediators used (450 μM) were neutral red (−330 mV) and methyl viologen (−430 mV); the reduction potentials of the mediators at pH 7 are indicated in parentheses. The ambient redox potentials were adjusted by using a solution of 1 mM sodium dithionite and were measured with a platinum electrode (M21PT) and a Ag/AgCl reference electrode (REF201), both purchased from Radiometer Copenhagen. The vessel was continuously flushed with deoxygenated argon. At the respective potentials, 200 μL aliquots were transferred under anoxic conditions into an EPR tube and subsequently frozen in liquid nitrogen. The redox potentials are relative to the normal hydrogen electrode.

Mössbauer Spectroscopy. For Mössbauer measurements, [^{57}Fe]FhuF was isolated from *E. coli* grown in [^{57}Fe]-rich medium as described in ref *9*. The Mössbauer spectra of frozen samples were recorded in the horizontal transmission geometry using a constant acceleration spectrometer operated in conjunction with a 512-channel analyzer in the time scale mode. The source was at room temperature and consisted of 0.93 GBq [^{57}Co] diffused in Rh foil (Cyclotron Co. Ltd., Obninsk, Russia). The spectrometer was calibrated against a metallic α-iron foil at room temperature, yielding a standard line width of 0.24 mm s^{-1}. The Mössbauer cryostat was a helium bath cryostat (MD306; Oxford Instruments). A small field of 20 mT perpendicular to the γ-beam was applied to the tail of the bath cryostat using a permanent magnet. Preliminary spectroscopic parameters have been reported earlier (*9*).

RESULTS

Transport and Iron Release. Reductive iron removal from [Fe^{3+}] siderophores is in general a rapid process (*1*, *3*, *12*, *13*). If FhuF were involved in siderophore reduction, higher amounts of [$^{55}Fe^{3+}$] siderophores should be observed in a *fhuF* mutant than in the *fhuF*$^+$ parental strain. If the reduction and the mobilization of iron in the cytoplasm is slowed by the lack of FhuF, the [Fe^{3+}] siderophore should accumulate in the mutant strain. To test this hypothesis, after 16 min of [^{55}Fe] siderophore uptake, various siderophores were extracted from whole cells with benzyl alcohol, which has been used to extract hydrophobic siderophore−iron complexes from fermentation broths and mycelia (*14*). Cytoplasmic metabolism of the [$^{55}Fe^{3+}$] siderophores ferrioxamine B, ferrichrome, coprogen, aerobactin, and enterobactin was tested (Table 2).

Transport assays with ferrioxamine B showed very little uptake (data not shown). To enhance ferrioxamine B transport, plasmid pFU2 encoding the ferrioxamine B FoxA receptor of *Yersinia enterocolitica* (*15*) was introduced into *E. coli* H1443 and into the *fhuF* mutant H1717. When [^{55}Fe]-ferrioxamine B was added to cells suspended in 5 M NaCl, 72% of the retained radioactivity could be extracted from whole cells. After 16 min transport of [^{55}Fe]ferrioxamine B, merely 4.6% of the [^{55}Fe] incorporated by *E. coli* H1443 (pFU2) could be extracted. In contrast, 25.4% of the [^{55}Fe] was extracted from the *fhuF* mutant H1717 (pFU2). This indicated that iron mobilization in the *fhuF* mutant was considerably slower than in the parent strain.

The extractable [^{55}Fe] was also determined in the same strains after ferrichrome transport. Again, more [^{55}Fe] was extracted from the *fhuF* mutant than from the parent strain, which indicated that FhuF is also involved in the mobilization of iron from ferrichrome. The slower reduction has no observable consequences for growth since *fhuF* mutants grew as fast as the *fhuF*$^+$ parent strains on ferrichrome as the sole iron source. With the strain pair H1085 and H1608 *fhuF*, both derived from *E. coli* AB2847, similar higher amounts of [^{55}Fe] were extracted from the *fhuF* mutant after ferrichrome transport. For the uptake of [Fe^{3+}] via enterochelin

Table 2: Iron Siderophores Extracted from Whole Cells[a]

strain	relevant genes	siderophore	iron taken up in 15 min (pmol/10^9 cells)	% extracted	control % extractable
H1443 pFU2	*foxA*$^+$	ferrioxamine B	26.4	4.6 ± 1.5	72
H1717 pFU2	*foxA*$^+$ *fhuF*	ferrioxamine B	29.9	33.8 ± 0.4	
H1443 pFU2		ferrichrome	93	7.8 ± 0.6	97
H1717 pFU2	*fhuF*	ferrichrome	173	26.3 ± 1.7	
H1085		ferrichrome	303	3.2 ± 0.3	
H1608	*fhuF*	ferrichrome	165	24.8 ± 2.3	
H1004	*fes*	ferrichrome	224	2.2 ± 0.1	
H1443		coprogen	395	27 ± 1.3	94
H1717	*fhuF*	coprogen	366	42.9 ± 1.5	
H1443 pEN7	*iutA*$^+$	aerobactin[b]	293	4.3 ± 0.1	66
H1717 pEN7	*iutA*$^+$ *fhuF*	aerobactin	278	5.9 ± 0.2	
H1443 (MC)		enterochelin	205	2.6 ± 0.4	88
H1717 (MC)	*fhuF*	enterochelin	168	2.2 ± 0.3	

[a] $[^{55}Fe]^{3+}$ siderophores were transported for 16 min by the strains listed. Cells were extracted with 500 μL of benzyl alcohol. The amount of iron taken up after 15 min by $\sim 10^9$ cells is given. The percentage of radioactive [^{55}Fe] extractable with benzyl alcohol was determined. In the control column the percentage of [^{55}Fe] siderophore extractable from 50 μL of a cell suspension in 5 M NaCl and of labeled siderophore without transport is given. The relevant genes encode FoxA ferrioxamine outer membrane receptor for efficient ferrioxamine uptake, Fes enterochelin esterase, necessary for iron−enterochelin utilization, and IutA outer membrane aerobactin receptor, allows uptake of aerobactin by *E. coli* K-12. [b] Acidic extraction conditions were used for aerobactin: 5 M NaCl, 0.2 M glycine, and 0.1 M HCl.

(enterobactin), a functional Fes protein, which hydrolyzes enterochelin, is necessary for iron mobilization. As expected, no difference in the amount of extracted [^{55}Fe], provided as a ferrichrome complex, was observed between a *fes*$^+$ and a *fes* strain, which indicated that Fes is not involved in iron mobilization from ferrichrome.

Higher amounts of [^{55}Fe] were extracted from *E. coli* H1443 after coprogen-mediated transport as compared to after ferrichrome-mediated transport, which suggested a lower affinity of the reductase for ferrichrome. Nonetheless, nearly twice as much [^{55}Fe] was extracted from *E. coli* H1717 *fhuF*, which again indicated a slower mobilization of siderophore-bound iron in the mutant. Aerobactin, another siderophore used by *E. coli*, was extracted more efficiently after acidification of the cell suspension. Slightly more [^{55}Fe] was extracted from the *fhuF* mutant. There were no differences in the amount of [^{55}Fe] extracted after enterochelin-mediated iron transport in the *fhuF* mutant and parental strain. In a *fes* mutant, more than 70% of the transported [^{55}Fe] could be extracted; however, the amount of [^{55}Fe]enterobactin taken up by the *fes* mutant was very low, which precluded a direct comparison to the parental strain.

Determination of the Midpoint Potential of FhuF Using EPR Redox Titrations. If FhuF is part of a siderophore−reductase system, a redox potential of the [2Fe-2S] protein enabling reduction of the siderophore-bound ferric iron would be expected. An EPR redox titration experiment was used to determine the redox potential of FhuF. The EPR spectrum of the sodium dithionite-reduced protein showed a nearly axial EPR signal in the $g = 2$ region, typical of an $S = {}^1/_2$ system (Figure 1; $g_z = 1.994$, $g_y = 1.961$, and $g_x = 1.886$). The g_y value is within the range found for [2Fe-2S] clusters, whereas the g_z value is atypical of this cluster type. The values also do not match those of Rieske proteins ($g_z = 2.03$, $g_y = 1.89-1.9$, and $g_x = 1.78$). Details of the analysis of the EPR and Mössbauer spectroscopy studies will be published elsewhere. The focus here is on the EPR spectroscopic determination of the midpoint potential of FhuF and on the Mössbauer spectroscopic observation of the siderophore−FhuF redox couple. On the basis of a comparison of

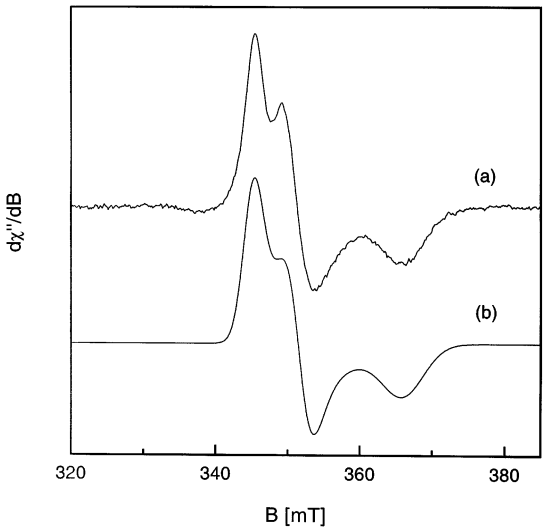

FIGURE 1: (a) X-band EPR spectrum of the sodium dithionite-reduced protein. Experimental conditions: microwave frequency, 9.6437 GHz; microwave power, 20 μW; attenuation, 40 dB; temperature, 30.0 K; modulation amplitude, 5 G; modulation frequency, 100 kHz. (b) The solid line is a theoretical simulation of the experimental spectrum with g-values $g_z = 1.994$, $g_y = 1.961$, and $g_x = 1.886$.

the EPR signal intensities of the fully reduced [2Fe-2S] protein with the intensities obtained at various potentials in the range from −240 to −460 mV relative to the normal hydrogen electrode, the redox potential of FhuF was determined to be $E_{1/2} = -310 \pm 25$ mV (see Figure 2). This redox potential is well within the range found for this class of proteins (−175 to −460 mV) (*16*). The redox potential of ferrioxamine B, coprogen, and ferrichrome is −468 ± 15 mV (*17*, *18*), −447 ± 7 mV (*19*), and −400 ± 10 mV (*20*), respectively. According to the Nernst equation, the effective range for a thermodynamically favorable redox reaction is ±59 mV with respect to the corresponding reduction potential. If, in addition, the uncertainty of the experimental data is taken into account, it is apparent that reduction of coprogen and of ferrichrome can be easily achieved, whereas for ferrioxamine B, reduction via FhuF

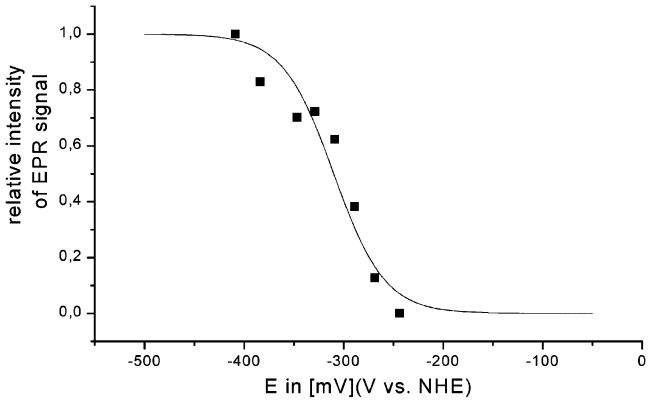

FIGURE 2: EPR reductive titration of FhuF under inert gas against a $Ag^+/AgCl$ electrode employing redox mediators (neutral red, methyl viologen) and an increasing amount of reductant (sodium dithionite, $K_3[Fe(CN)_6]$ in Tris-HCl, pH 7.3). When the reaction mixture was at specific potentials, approximately 200 μL of the reaction mixture was transferred under inert gas into an EPR tube. The tube was immediately frozen to 77 K and kept at this temperature until measurement. The potential-dependent increase of the $g = 2$ signal was used to estimate the redox potential of FhuF. The increase of signal intensity at $g = 2$ is shown in relation to the reduction potential created in the reaction vessel.

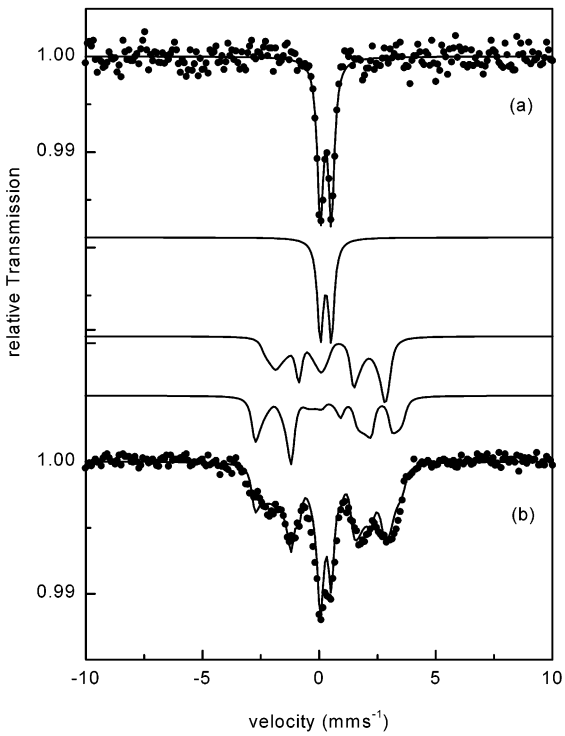

FIGURE 3: Mössbauer spectra of (a) the as-isolated [^{57}Fe]protein (frozen solution) and (b) the dithionite-reduced sample measured at 4.2 K in a field of 20 mT perpendicular to the γ-beam. Spectrum b consists of three subspectra, represented by solid lines corresponding to simulations based on a spin Hamiltonian (from top to bottom): (1) as-isolated (oxidized) protein (1.4 μmol); (2) reduced cluster, ferrous ion site; and (3) reduced cluster, ferric ion site. The reduced sample contains a portion of the as-isolated protein because the reduction was not complete (FhuF, 1.4 μmol; dithionite, 1.1μmol; volume, 900 μL). Complete reduction was avoided to prevent an excess of reductant in the solution. These conditions were required for the experiment, the results of which are shown in Figure 5. Mössbauer parameters are listed in Table 3.

is difficult (the highest potential that can be assumed for FhuF and the lowest value for ferrioxamine B is −394 mV). Therefore, direct evidence for ferrioxamine B reduction via FhuF is essential to prove the reductase function of FhuF.

Mössbauer Spectroscopic Analysis of the Ferrioxamine B/FhuF Redox Couple. Mössbauer spectroscopy is an excellent tool for determining the iron redox states of a compound or of a mixture of compounds of interest (*21*). Spectrum a in Figure 3 shows the Mössbauer spectrum of isolated [^{57}Fe]-FhuF in the oxidized state measured at 4.3 K. The corresponding Mössbauer parameters derived from least-squares fits employing Lorentzians are listed in Table 3. The isomer shift is typical of oxidized [2Fe-2S] proteins. The quadrupole splitting, however, is unusually low. For activation of [^{57}Fe]-FhuF, the oxidized as-isolated protein (1.4 mM) was reduced with sodium dithionite (1.1 mM final concentration in the reaction mixture in 10 mM MOPS buffer, pH 7.4). To avoid excess reductant, the molar ratio of FhuF:dithionite was kept at approximately 0.8; otherwise, reduction of ferrioxamine B-bound iron via FhuF would have been obscured (Figure 5).

Spectrum b in Figure 3 displays the partially reduced [^{57}Fe]-FhuF protein. The spectrum is composed of three subspectra represented by solid lines corresponding to simulations based on a spin Hamiltonian: (i) a portion of the starting material (as-isolated [^{57}Fe]FhuF which has not reacted), (ii) the ferric ion site of the reduced cluster, and (iii) the ferrous iron site of the reduced cluster.

Figure 4 represents the Mössbauer spectrum of an aqueous solution of 100 mM BSA and 12 mM ferric [^{57}Fe]ferrioxamine B. BSA was added as a spin dilutant to eliminate spin−spin relaxation. The spectrum is typical of a high-spin ferric ion in an octahedral oxygen environment under conditions of slow spin−spin relaxation. The solid line in Figure 4 represents a simulation based on a spin Hamiltonian

Table 3: Mössbauer Parameters of FhuF and Ferrioxamine B[a]

	δ[b] (mm s^{-1})	ΔE_Q[c] (mm s^{-1})	Γ[d] (mm s^{-1})	relative area (%)
protein as isolated (Figure 3a)	0.29 ± 0.02	0.47 ± 0.04	0.31 ± 0.02	100
protein reoxidized by ferrioxamine B (Figure 5)	0.28 ± 0.02	0.47 ± 0.03	0.28 ± 0.02	45
$Fe(H_2O)_6^{2+}$ released from ferrioxamine B (Figure 5)	1.30 ± 0.02	3.04 ± 0.05	0.48 ± 0.02	55
reduced FhuF−Fe^{2+} (Figure 3b)	0.65 ± 0.02	2.93 ± 0.04	0.35 ± 0.03	39
reduced FhuF−Fe^{3+} (Figure 3b)	0.35 ± 0.02	0.94 ± 0.03	0.35 ± 0.03	39
residual as-isolated FhuF (Figure 3b)	0.29 ± 0.03	0.47 ± 0.05	0.32 ± 0.02	22

[a] The iron cluster of FhuF was in the oxidized [Fe^{3+}-Fe^{3+}] and reduced [Fe^{2+}-Fe^{3+}] state as determined in spectra measured at 4.3 K in a field of 20 mT applied perpendicular to the γ-beam (see Figures 3 and 5). The iron of ferrioxamine B was reduced, typical of high-spin ferrous ion surrounded by an octahedral oxygen ligand sphere. The ferric site of the reduced cluster exhibited isotropic hyperfine coupling constants: $A_{xx}/g_N\mu_N = A_{yy}/g_N\mu_N = A_{zz}/g_N\mu_N = -35.6 \pm 1$ T. Those of the ferrous site were anisotropic: $A_{xx}/g_N\mu_N = 29.7 \pm 1$ T, $A_{yy}/g_N\mu_N = 15.7 \pm 1$ T, and $A_{zz}/g_N\mu_N = -8.0 \pm 1$ T. [b] Isomer shift relative to α-iron at room temperature. [c] Quadrupole splitting. [d] Line width at half-height.

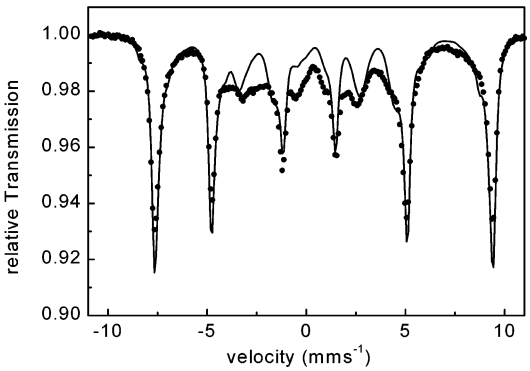

FIGURE 4: Mössbauer spectrum of a frozen aqueous solution of [$^{57}Fe^{3+}$]ferrioxamine B (12 mM) employing BSA (100 mM) as a dilutant to minimize spin−spin relaxation. The solid line represents a simulation based on a spin Hamiltonian: line width = 0.35 mm s^{-1}; zero-field splitting, $D = 1.2$ cm^{-1}; rhombicity parameter, $E/D = 0.33$; $\delta = 0.52$ mm s^{-1}; $\Delta E_Q = -0.84$ mm s^{-1}; asymmetry parameter, $\eta = 1$; and isotropic hyperfine coupling tensor, $A_{xx}/g_N\mu_N = A_{yy}/g_N\mu_N = A_{zz}/g_N\mu_N = -22.1$ T. The simulation does not completely fit the experimental data. This discrepancy is caused by relaxation effects that are not dealt with in the spin Hamiltonian simulation. The experimental conditions were as described in Figure 3.

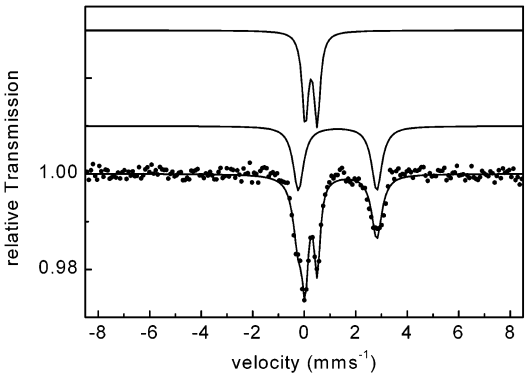

FIGURE 5: Mössbauer spectrum of FhuF (same sample as in Figure 3) mixed with [^{57}Fe]ferrioxamine B (1.2 μmol, final volume 1 mL). The experimental conditions were as described in Figure 3. To avoid excess reductant, the molar ratio of FhuF:dithionite was kept approximately at 0.8. FhuF was, therefore, merely partially reduced, while ferrioxamine B was fully oxidized before mixing. The spectrum consists of two subspectra represented by solid lines (from top to bottom): (1) as-isolated (oxidized) protein and (2) [Fe-$(H_2O)_6]^{2+}$ released from ferrioxamine B. The spectrum shows that FhuF is fully oxidized. Iron from ferrioxamine B is fully reduced. All measurements were performed in the presence of a magnetic field of 20 mT oriented perpendicular to the γ-beam. The corresponding Mössbauer parameters are listed in Table 3.

(line width, 0.35 mm s^{-1}; zero-field splitting, $D = 1.2$ cm^{-1}; rhombicity parameter, $E/D = 0.33$; $\delta = 0.52$ mm s^{-1}; $\Delta E_Q = -0.84$ mm s^{-1}; asymmetry parameter, $\eta = 1$; and isotropic hyperfine coupling tensor, $A_{xx}/g_N\mu_N = A_{yy}/g_N\mu_N = A_{zz}/g_N\mu_N = -22.1$ T). The simulation does not fit the experimental data completely. This discrepancy is caused by relaxation effects that are not dealt with in the spin Hamiltonian simulation. The Mössbauer parameters of [^{57}Fe]ferrioxamine B based on our spin Hamiltonian analysis differed slightly from values reported earlier (*22*) ($\Delta E_Q = -0.84$ vs 0.77 mm s^{-1}). Approximately 10% of the [^{57}Fe]ferrioxamine B solution (100 μL, 1.2 μmol) was mixed with the partially reduced FhuF protein shown in Figure 3 under an argon atmosphere (final volume 1 mL). In the Mössbauer spectrum (Figure 5), two quadrupole doublets are visible. The Mössbauer parameters resulting from least-squares fits of Lorentzians are listed in Table 3.

A comparison with Figure 3a and the parameters derived from this spectrum revealed that [^{57}Fe]FhuF was converted to its fully oxidized [2Fe-2S] cluster form (45% of the absorption area). No residual ferric ferrioxamine B is detectable in the spectrum. Rather, a high-spin ferrous species in an octahedral oxygen environment is visible (Table 3, Figure 5, 55% of the absorption area). The Mössbauer spectrum reveals that (1) FhuF is capable of direct reduction of ferrioxamine B-bound ferric ion and (2) the reduced ferrous ion species is not bound to the [2Fe-2S] cluster and the cluster structure is not affected. Since FhuF itself requires a reductant for activation, it is not surprising that the reaction of FhuF with ferrioxamine B did not exhibit an equilibrium. Rather, a complete consumption of reduction equivalents was observed.

DISCUSSION

A prerequisite for siderophore reduction by FhuF is that the redox potentials of both partners are within the effective range for a thermodynamically favorable electron transfer which is ±59 mV with respect to the corresponding redox potentials (Table 4). These considerations make the reduction of aerobactin and ferrichrome by FhuF possible, while for coprogen one has to include the experimental errors to get a favorable overlap. Ferrioxamine B seems to be out of the favorable range with −394 mV, the value just reached also by FhuF under inclusion of the experimental error. However, it has been postulated that it is the redox potential of the reductase−ferric−siderophore association rather than the redox potential of the free ferric siderophore that is important when considering reduction as a process involved in iron release (*24*).

Table 4: Redox Potentials[a]

compound	redox potential (mV)	effective range (mV)[b]	ref
FhuF	−310 ± 25	−241 to −369	this work
aerobactin	−336	−277 to −395	*23*
ferrichrome	−400 ± 10	−341 to −459	*20*
coprogen	−447 ± 7	−388 to −506	*19*
ferrioxamine B	−468 ± 15	−409 to −527	*17*, *18*

[a] The redox potentials of the siderophores have been used to calculate the thermodynamically favorable range for an electron transfer. This effective range is further extended if the uncertainty of experimental data is taken into account. [b] In addition, the error margins of both FhuF and the corresponding siderophore have to be added in order to obtain the full possible range of a favorable redox reaction. In the case of ferrioxamine B, this would be −409 ± 15 to −527 ± 15 mV; in the case of FhuF, −241 ± 25 to −369 ± 25 mV.

Substantial indications for a role of FhuF in iron removal from siderophores came from [^{55}Fe]hydroxamate siderophore extraction experiments. These experiments uncovered a significant difference between *fhuF* mutants and their corresponding parental strains (Table 2). The data from *fhuF* mutants indicated that iron removal from the hydroxamate siderophores employed is clearly slower than in the corresponding parental strains. This implies that FhuF is involved in iron utilization from these hydroxamate siderophores. In fact, the FhuF−ferrioxamine B redox experiment (Table 3, Figures 3−5) clearly demonstrated the ferric siderophore

reductase function of the FhuF protein. The Mössbauer parameters of reoxidized FhuF are, within experimental error, the same as for the as-isolated protein. Therefore, it can be concluded that the cluster is not decomposed during the one-electron transfer process. Since siderophores have a much lower affinity for [Fe_{aq}^{2+}] than for [Fe_{aq}^{3+}], we assume that the ferrous iron formed is present mainly as an aquo complex. The reaction with ferrioxamine B (FoxB) can be, therefore, summarized as follows:

$$[2Fe\text{-}2S]FhuF^{1+} + [Fe]FoxB \rightarrow [2Fe\text{-}2S]FhuF^{2+} + [Fe_{aq}^{2+}] + FoxB^{3-}$$

It is not yet known which cellular system regenerates the FhuF reductase after electron transfer. Moreover, it has to be pointed out that the formation of bulk "free" [Fe_{aq}^{2+}] ferrous ion in vivo is not to be expected. [Fe_{aq}^{2+}] is Fenton active and thus deleterious to cells. Therefore, it is likely that the ferrous iron is bound by a chaperone-like structure or other novel structural elements to enable sheltered intracellular transfer of this ion. In fact, we have previously detected an oligomeric sugar phosphate in *E. coli* (*25*) that binds ferrous iron (cytoplasmic concentration: approximately 500 μM) intracellularly released from ferrichrome [*E. coli* (*4*)] or ferrioxamine E [*Pantoea agglomerans* (*3*)]. This compound was named ferrochelatin (*26*).

Finally, the different phenotypes observed under ferrichrome- or coprogen-controlled growth and under ferrioxamine B-controlled growth need to be explained in the light of the results reported herein. Growth promotion tests of *fhuF* mutants employing coprogen or ferrichrome as the sole iron source revealed growth rates similar to those of the *fhuF*$^+$ parental strains, which indicated sufficient iron supply. Although removal of iron from the siderophores was shown here to be slow, sufficient amounts of the metal ion could be utilized to prevent growth limitation. This was probably achieved via unspecific [Fe^{3+}] siderophore reduction by flavin reductases as described previously (*2*, *27*−*30*). Flavin reductases are not regulated by iron and usually reduce, under in vivo conditions, substrates other than [Fe^{3+}]. These general cellular redox systems are obviously able to reduce sufficient amounts of ferric iron from the siderophores coprogen and ferrichrome to prevent growth limitation. Under ferrioxamine B-controlled growth conditions, however, *fhuF* mutants failed to grow. The redox potential of ferrioxamine B is significantly lower than that of the other two siderophores. In *fhuF* mutants, the reduction potential of the nonspecific redox systems might be too high to mobilize sufficient amounts of ferrous iron, and hence, diminished growth and derepression of Fur-regulated iron transport systems was observed. In the parent strains, however, the presence of FhuF enables reductive mobilization of sufficient amounts of [Fe^{2+}] from ferrioxamine B. In summary, we showed that FhuF acts as a siderophore reductase. The corresponding process is specific since it is regulated by Fur. We suggest that the observed phenotypes and earlier observations point to additional unspecific siderophore reduction pathways, the efficacy of which depends on the redox potential of the siderophore.

The amino acid sequence of FhuF does not show significant similarities to sequences of known [2Fe-2S] proteins. However, in *Rhizobium leguminosarum* and in *Rhizobium meliloti*, a homologue of the *fhuF* gene is found directly downstream of a *fhuA* gene encoding a hydroxamate receptor protein (*31*, *32*). The level of identity of the predicted proteins with FhuF is rather low (∼20%); however, the characteristic CC motif and two additional cysteines are conserved in the C-terminus of these proteins. In *Vibrio parahaemolyticus* (*33*), a protein encoded upstream of *iutA*, which encodes the receptor protein for aerobactin, has been identified; the protein shares similarities with AlcD, which is located in a *Bordetella pertussis* operon responsible for the synthesis of the siderophore alcaligin (*34*). The function of these two proteins is not known. However, since they have the same cysteine pattern as FhuF, also these proteins might have a siderophore reductase function and together with FhuF constitute a novel class of enzymes.

ACKNOWLEDGMENT

We thank Karen A. Brune (Marburg) and Volkmar Braun (Tübingen) for critical reading of the manuscript.

REFERENCES

1. Wilkins, R. G. (1991) *Kinetics and mechanisms of reactions of transition metal complexes*, 2nd ed., VCH, Weinheim, Germany.
2. Fontecave, M., Coves, J. and Pierre, J. L. (1994) Ferric reductases or flavin reductases?, *BioMetals 7*, 3−8.
3. Matzanke, B. F., Berner, I., Bill, E., Trautwein, A. X., and Winkelmann, G. (1991) Transport and utilization of ferrioxamine-E-bound iron in *Erwinia herbicola* (*Pantoea agglomerans*), *BioMetals 4*, 181−185.
4. Matzanke, B. F., Müller, G. I., Bill, E., and Trautwein, A. X. (1989) Iron metabolism of *Escherichia coli* studied by Mössbauer spectroscopy and biochemical methods, *Eur. J. Biochem. 183*, 371−379.
5. Hartmann, A., Fiedler, H. P., and Braun, V. (1979) Uptake and conversion of the antibiotic albomycin by *Escherichia coli* K-12, *Eur. J. Biochem. 99*, 517−524.
6. Sauer, M., Hantke, K., and Braun, V. (1987) Ferric-coprogen receptor FhuE of *Escherichia coli*: processing and sequence common to all TonB-dependent outer membrane receptor proteins, *J. Bacteriol. 169*, 2044−2049.
7. Rohrbach, M. R., Braun, V., and Köster, W. (1995) Ferrichrome transport in *Escherichia coli* K-12: altered substrate specificity of mutated periplasmic FhuD and interaction of FhuD with the integral membrane protein FhuB, *J. Bacteriol. 177*, 7186−7193.
8. Zheng, M., Wang, X., Doan, B., Lewis, K. A., Schneider, T. D., and Storz, G. (2001) Computation-directed identification of OxyR DNA binding sites in *Escherichia coli*, *J. Bacteriol. 183*, 4571−4579.
9. Müller, K., Matzanke, B. F., Schünemann, V., Trautwein, A. X., and Hantke, K. (1998*)* FhuF, an iron-regulated protein of *Escherichia coli* with a new type of [2Fe-2S] center, *Eur. J. Biochem. 258*, 1001−1008.
10. Miller, J. H. (1972) *Experiments in molecular genetics*, Cold Spring Harbor Laboratory, Cold Spring Harbor, NY.
11. Dutton, P. L. (1978) Redox potentiometry: determination of midpoint potentials of oxidation−reduction components of biological electron-transfer systems, *Methods Enzymol. 54*, 411−435.
12. Matzanke, B. F., Bill, E., Trautwein, A. X., and Winkelmann, G. (1990) Siderophores as storage compounds in the yeast *Rhodotorula minuta* and *Ustilago sphaerogena* detected by Mössbauer spectroscopy, *Hyperfine Interact. 58*, 2359−2364.
13. Rauscher, L., Expert, D., Matzanke, B. F., and Trautwein, A. X. (2002) Chrysobactin-dependent iron acquisition in *Erwinia chrysanthemi*. Functional study of a homologue of the *Escherichia coli* ferric enterobactin esterase, *J. Biol. Chem. 277*, 2385−2395.
14. Winkelmann, G. (1986) Iron complex products (siderophores), in *Biotechnology* (Rehm, H. J., and Reed, G., Eds.) Vol. 4, pp 216−243, VCH, Weinheim, Germany.
15. Bäumler, A. J., and Hantke, K. (1992) Ferrioxamine uptake in *Yersinia enterocolitica*: characterization of the receptor protein FoxA, *Mol. Microbiol. 6*, 1309−1321.

16. Stephens, P. J., Jollie, D. R., and Warshel, A. (1996) Protein control of redox potentials of iron−sulfur proteins, *Chem. Rev. 96*, 2491−2513.
17. Bickel, H., Hall, G. E., Keller-Schierlein, W., Prelog, V., Vischer, E., and Wettstein, A. (1960) Stoffwechselprodukte von Actinomyceten, 27. Mitt. Über die Konstitution von Ferrioxamin B, *Helv. Chim. Acta 43*, 2129−2138.
18. Cooper, S. R., McArdle, J. V., and Raymond, K. N. (1978) Siderophore electrochemistry: relation to intracellular iron release mechanism, *Proc. Natl. Acad. Sci. U.S.A. 75*, 3551−3554.
19. Wong, G. B., Kappel, M. J., Raymond, K. N., Matzanke, B., and Winkelmann, G. (1983) Coordination chemistry of microbial iron transport compounds. 24. Characterization of coprogen and ferricrocin, two ferric hydroxamate siderophores, *J. Am. Chem. Soc. 105*, 810.
20. Wawrousek, E. F., and McArdle, J. V. (1982) Spectrochemistry of ferrioxamine B, ferrichrome, and ferrichrome A, *J. Inorg. Biochem. 17*, 169−183.
21. Matzanke, B. F. (1991) Structures, coordination chemistry and functions of microbial iron chelates, in *CRC handbook of microbial iron chelates* (Winkelmann, G., Ed.) pp 15−64, CRC Press, Boca Raton, FL.
22. Bock, J. L, and Lang, G. (1972) Mossbauer spectroscopy of iron chelated by deferoxamine, *Biochim. Biophys. Acta 264*, 245−251.
23. Harris, W. R., Carrano, C. J., and Raymond, K. N. (1979) Isolation, characterization and formation constants of aerobactin, *J. Am. Chem. Soc. 101*, 2722−2727.
24. Neilands, J. B. (1995) Siderophores: structure and function of microbial iron transport compounds, *J. Biol. Chem. 270*, 26723−26726.
25. Böhnke, R., and Matzanke, B. F. (1995) The mobile ferrous iron pool in *Escherichia coli* is bound to a phosphorylated sugar derivative, *BioMetals 8*, 223−230.
26. Matzanke, B. F. (1997) Iron storage in microorganisms, in *Transition Metals in Microbial Metabolism* (Winkelmann, G., and Carrano, C. J., Eds.) pp 117−157, Harwood Academic Publishers, Amsterdam, The Netherlands.
27. Ernst, J. F., and Winkelmann, G. (1977) Enzymatic release of iron from sideramines in fungi. NADH:sideramine oxidoreductase in *Neurospora crassa*, *Biochim. Biophys. Acta 500*, 27−41.
28. Arceneaux, J. E. L., and Byers, B. R. (1980) Ferrisiderophore reductase activity in *Bacillus megaterium*, *J. Bacteriol. 141*, 715−721.
29. McCready, K. A., and Ratledge, C. (1979) Ferrimycobactin reductase activity from *Mycobacterium smegmatis*, *J. Gen. Microbiol. 113*, 67−73.
30. Fischer, E., Strehlow, B., Hartz, D., and Braun, V. (1990) Soluble and membrane-bound ferrisiderophore reductases of *Escherichia coli* K-12, *Arch. Microbiol. 153*, 329−336.
31. Capela, D., Barloy-Hubler, F., Gouzy, J., Bothe, G., Ampe, F., Batut, J., Boistard, P., Becker, A., Boutry, M., Cadieu, E., Dreano, S., Gloux, S., Godrie, T., Goffeau, A., Kahn, D., Kiss, E., Lelaure, V., Masuy, D., Pohl, T., Portetelle, D., Puehler, A., Purnelle, B., Ramsperger, U., Renard, C., Thebault, P., Vandenbol, M., Weidner, S., and Galibert, F. (2001) Analysis of the chromosome sequence of the legume symbiont *Sinorhizobium meliloti* strain 1021, *Proc. Natl. Acad. Sci. U.S.A. 98*, 9889−9894.
32. GenBank Accession Number AJ3155451.
33. Funahashi, T., Tanabe, T., Aso, H., Nakao, H., Fujii, Y., Okamoto, K., Narimatsu, S., and Yamamoto, S. (2003) An iron-regulated gene required for utilization of aerobactin as an exogenous siderophore in *Vibrio parahaemolyticus*, *Microbiology 149*, 1217−1225.
34. Pradel, E., Guiso, N., and Locht, C. (1998) Identification of AlcR, an AraC-type regulator of alcaligin siderophore synthesis in *Bordetella bronchiseptica* and *Bordetella pertussis*, *J. Bacteriol. 180*, 871−880.
35. Braun, V., Günthner, K., Hantke, K., and Zimmermann, L. (1983) Intracellular activation of albomycin in *Escherichia coli* and *Salmonella typhimurium*, *J. Bacteriol. 156*, 308−315.

BI0357661